Res Chem Intermed
DOI 10.1007/s11164-014-1889-x

New biscoumarin and dihydropyran derivatives as antimicrobials

Jing Li · Jing-ru Meng · Di Qu · Zi-dan Zhang · Fen Li · Xiao-hui Yang · Xiao-xing Luo · Jiang-tao Li · Ming-kai Li

Received: 22 September 2014 / Accepted: 1 December 2014

Abstract In an attempt to find a new class of antimicrobial agents, a series of biscoumarin (1–4) and dihydropyran (5 and 6) derivatives were prepared. These compounds were screened for their in vitro antibacterial activity against *Staphylococcus aureus* (*S. aureus* ATCC 29213), methicillin-resistant *S. aureus* (MRSA XJ 75302), vancomycin-intermediate *S. aureus* (Mu50 ATCC 700699), and USA 300 (Los Angeles County clone, LAC). There are two classical intramolecular O–H···O hydrogen bonds (HBs) in the structures of biscoumarins 1–4 and the corresponding total HB energy were further performed with the density functional theory (DFT) [B3LYP/6-31G*] method.

Keywords Biscoumarin · Dihydropyran · *Staphylococcus aureus* · Minimum inhibitory concentration

Jing Li and Jing-ru Meng contributed equally to this work.

J. Li · X. Yang · J. Li (✉)
College of Chemistry and Chemical Engineering, The Key Laboratory for Surface Engineering and Remanufacturing in Shaanxi Province, Xi'an University, Xi'an, China
e-mail: lijiangtao-968@xawl.edu.cn

J. Meng · D. Qu · F. Li · X. Luo · M. Li (✉)
Department of Pharmacology, School of Pharmacy, the Fourth Military Medical University, Xi'an, China
e-mail: mingkai@fmmu.edu.cn

Z. Zhang
Department of Physics, School of Science, Tianjin University, Tianjin, China

Published online: 06 January 2015

Introduction

Staphylococcus aureus (*S. aureus*) is a major pathogen that leads to various of healthcare-associated infections, and has become a more significant clinical problem because of resistance to almost all the anti-bacterial agents [1–3]. Naturally occurring strains of methicillin-resistant *Staphylococcus aureus* (MRSA), which was first reported from England in 1961 [4], has resulted in the cause of major outbreaks and epidemics in hospitalized patients. Vancomycin is currently the most effective antibiotic treatment for MRSA [5]. However, the emergence of MARS with decreased susceptibility to vancomycin induced to the urgent necessity of developing new antimicrobials [6, 7].

Because of different substituents on the central linker methylene leading to chemical modifications, biscoumarin and dihydropyran derivatives have revealed promising biological activity with interesting potential in therapeutic application besides their traditional use as anticoagulants, antifungal, anti-inflammatory agents, etc. [8, 9]. They have also shown important properties as antibiotics (novobiocin and analogs), anti-AIDS agents (calanolides), and antitumor drugs [10, 11].

Therefore, in light of the above facts, we have successfully synthesized four biscoumarins (1–4) and two dihydropyrans (5 and 6) (Fig. 1), and all the final synthesized compounds were tested for their antibacterial activities. Additionally, for biscoumarins 1–4, their total HB energies were calculated by density functional theory (DFT) method.

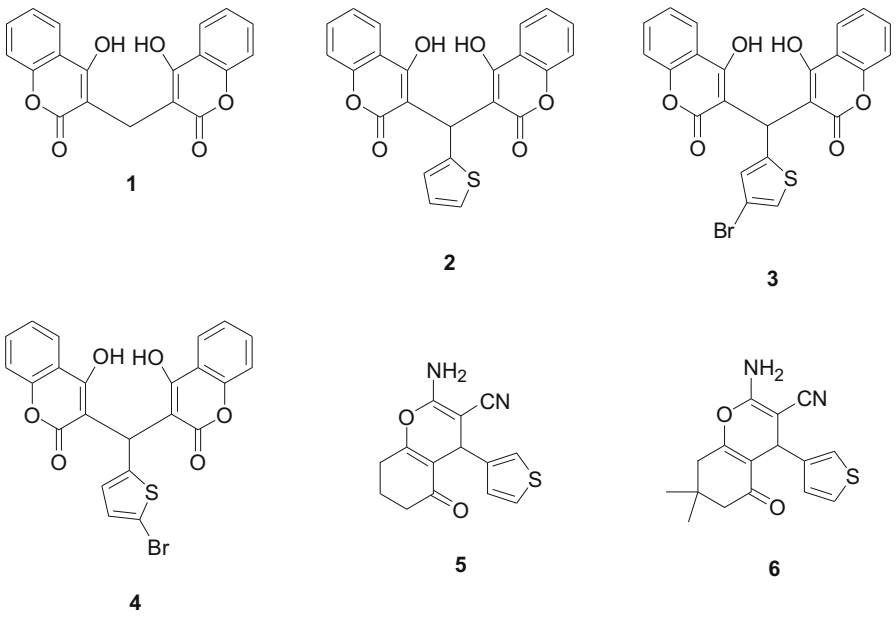

Fig. 1 Chemical structures of compounds 1–6

Experimental

Apparatus and materials

IR spectra (400–4,000 cm^{-1}) were obtained using a Bruker Equinox-55 spectrophotometer. ^1H NMR spectra were obtained using a Varian Inova-400 spectrometer (at 400 MHz). Mass spectra were obtained using a micrOTOF-Q II mass spectrometer. The melting points were taken on a XT-4 micro melting apparatus, and the thermometer was uncorrected.

All antibiotics used were purchased from the National Institute for the Control of Pharmaceutical and Biological Products (Beijing, China). All other chemicals and solvents were of analytical grade.

MRSA (XJ 75302) was isolated from cultures of sputum samples from patients in Xijing Hospital (Xi'an, China). *S. aureus* strain (ATCC 29213) was purchased from the Chinese National Center for Surveillance of Antimicrobial Resistance. Mu50 (ATCC 700699) and USA 300 (LAC) were purchased from MicroBiologics (MN, USA).

Synthesis and characterization of compounds 1–6

Compounds 1–4 were synthesized according to the methods of a previous report [12]. A mixture of formaldehyde (or thiophene-2-carbaldehyde, 4-bromo-thiophene-2-carbaldehyde and 5-bromo-thiophene-2-carbaldehyde) (10 mmol) and 4-hydroxycoumarin (20 mmol) was dissolved in 100 ml of EtOH. A few drops of piperidine were added, and the mixture was stirred for 3 h at room temperature. After reaction completion as determined by TLC, water was added until precipitation occurred. After filtering the precipitates, they were sequentially washed with ice-cooled water and ethanol and then dried in a vacuum.

3,3′-Methylenedi(4-hydroxycoumarin) (1): m.p. 289–290 °C. IR(KBr pellet cm^{-1}): 3051(OH), 1645(CO), 1526(C = C). ^1H NMR ($CDCl_3$, δ, ppm): 11.322(s, 2H), 7.988–8.011(q, 2H), 7.571–7.614(m, 2H), 7.347–7.393(m, 4H), 3.847(s, 2H). HRMS (ESI^+): *m/z*: calcd for [$C_{19}H_{12}O_6 + Na^+$]: 359.0526; found: 359.0544.

3,3′-(2-Thienyl-methylene)-bis-(4-hydroxycoumarin) (2): m.p. 206–207 °C. IR(KBr pellet cm^{-1}): 1,665, 1,612, 1,567, 1,514, 1,356, 767 cm^{-1}. ^1H NMR ($CDCl_3$, δ, ppm): 11.803(s, 1H), 11.290(s, 1H), 8.017–8.073(m, 2H), 7.617–7.656(q, 2H), 7.399–7.420(d, 4H), 7.214–7.227(d, 1H), 6.940–6.962(t, 1H), 6.855–6.864(t, 1H), 6.200(s, 1H). HRMS (ESI^+): *m/z*: calcd for [$C_{23}H_{14}SO_6 + Na^+$]: 441.0403; found: 441.0411.

3,3′-(4-Bromo-2-thienyl-methylene)-bis-(4-hydroxycoumarin) (3): m.p. 207–208 °C. IR(KBr pellet cm^{-1}): 1,666, 1,620, 1,571, 1,533, 1,363, 1,246, 1,143, 911, 760 cm^{-1}. ^1H NMR ($CDCl_3$, *δ*, ppm): 11.871(s, 1H), 11.307(s, 1H), 8.045–8.090(t, 2H), 7.651–7.690(t, 2H), 7.422–7.443(d, 4H), 7.144(s, 1H), 6.789(s, 1H), 6.169(s, 1H). HRMS (ESI^+): *m/z*: calcd for [$C_{23}H_{13}BrO_6S + Na^+$]: 518.9508; found: 518.9532.

3,3′-(5-Bromo-2-thienylmethylene)-bis-(4-hydroxycoumarin) (4): m.p. 217–218 °C. IR(KBr pellet cm^{-1}): 1,673, 1,620, 1,552, 1,492, 1,356, 1,318, 1,205, 1,099, 971, 767 cm^{-1}. ^1H NMR ($CDCl_3$, δ, ppm): 11.890(s, 1H), 11.299(s, 1H), 8.036–8.090(q, 2H), 7.646–7.685(t, 2H), 7.420–7.441(d, 4H), 6.910–6.919(d, 1H), 6.634–6.647(q, 1H), 6.118–6.122(d, 1H). HRMS (ESI^+): *m/z*: calcd for [$C_{23}H_{13}BrO_6S + Na^+$]: 518.9508; found: 518.9589.

Dihydropyran derivatives (5 and 6) were also synthesized according to a reported procedure [13]. A mixture of 3,5-cyclohexanedione (1,1-dimethyl-3,5-cyclohexanedione) (10 mmol), thiophene-3-carbaldehyde (10 mmol), malononitrile (10 mmol) and 4-(dimethylamino)pyridine (DMAP) (1 mmol) in ethanol (100 ml) was refluxed for 2–3 h and then cooled to room temperature. After filtering the precipitates, they were sequentially washed with ice-cooled water and ethanol and then dried under a vacuum.

2-Amino-4-(3-thienyl)-5-oxo-5,6,7,8-tetrahydro-4*H*-chromene-3-carbonitrile (5): m.p. 196–197 °C. IR(KBr pellet cm^{-1}): 3,311, 3,174, 2,191, 1,654, 1,365, 1,213, 997, 765 cm^{-1}. ^1H NMR (DMSO-d_6, δ, ppm): 7.412–7.432 (q, 1H), 7.133–7.143 (q, 1H), 7.028 (s, 2H), 6.903–6.919 (q, 1H), 4.317 (s, 1H), 2.574–2.601 (t, 2H), 2.299–2.323 (t, 2H), 1.894–1.984 (m, 2H). HRMS (ESI^+): *m/z*: calcd for [$C_{14}H_{12}N_2O_2S + Na^+$]: 295.0512; found: 295.0554.

2-Amino-4-(3-thienyl)-3-cyano-7,7-dimethyl-5-oxo-4H-5,6,7,8-tetrahydrobenzo[b]pyran (6): m.p. 225–226 °C. IR(KBr pellet cm^{-1}): 3,383, 3,207, 2,191, 1,670, 1,606, 1,365, 1,213, 1,133, 1,038, 765 cm^{-1}. ^1H NMR (DMSO-d_6, δ, ppm): 7.412–7.432 (q, 1H), 7.133–7.143 (q, 1H), 7.028 (s, 2H), 6.903–6.919 (q, 1H), 4.317 (s, 1H), 2.574–2.601 (t, 2H), 2.299–2.323 (t, 2H), 1.894–1.984 (m, 2H). HRMS (ESI^+): *m/z*: calcd for [$C_{16}H_{16}N_2O_2S + Na^+$]: 323.0825; found: 323.0833.

X-ray crystallography

For X-ray diffraction experiments, single crystals of compounds 4 and 6 were both grown from methanol. The X-ray diffraction data were collected on a Bruker SMART APEX II CCD diffractometer equipped with a graphite monochromated Mo-Kα radiation ($\lambda = 0.71073$ Å) by using the ω-2θ scan technique at room temperature. The structure was solved by direct methods using SHELXS-97 [14] and refined using the full-matrix least squares method on F^2 with anisotropic thermal parameters for all non-hydrogen atoms by using SHELXL-97. Hydrogen atoms were generated geometrically. The crystal data and details concerning data collection and structure refinement are given in Table 1. Molecular illustrations were prepared using the XP package. Parameters in CIF format are available as Electronic Supplementary Publication from Cambridge Crystallographic Data Centre.

Quantum chemical calculations

All calculations were carried out using the Gaussian 09 package [15]. Density functional theory [16], Becke's three-parameter hybrid function (B3LYP) [17], and LYP correlation function [18] were used to fully optimize all of the geometries on the energy surface without constraints. To obtain precise results that are in conjunction

Table 1 Crystal data, data collection, and structure refinement

	Compound 4	Compound 6
Formula	$C_{23}H_{13}BrO_6S$	$C_{16}H_{16}N_2O_2S$
*M*r	497.30	300.0932
Crystal system	Monoclinic	Monoclinic
Space group	$P2_1/c$	$P2_1/c$
a/Å	9.8301 (6)	11.3333 (6)
b/Å	10.2686 (9)	9.2903 (7)
c/Å	20.3329 (15)	14.6589 (10)
α/°	90	90
β/°	95.321 (5)	98.658 (5)
γ/°	90	90
V/Å^3	2,043.6 (3)	1,525.84 (17)
Z	4	4
D_{calc}/g cm^{-3}	1.616	1.299
μ (Mo Kα)/mm^{-1}	2.153	0.217
θ range/°	2.76 to 25.00	2.60 to 25.00
Reflections collected	7,159	6,261
No. unique data [*R*(int)]	3,596 [0.0235]	2,681 [0.0294]
No. data with $I \geq 2\sigma(I)$	2,376	1,921
R_1	0.0648	0.1382
ωR_2 (all data)	0.2030	0.3900
CCDC	1,017,804	1,035,052

with experimental results, three basis sets, namely 6-31G*, 6-31 + G**, and 6-311G*, were tested. Frequency calculations at the B3LYP (with basis sets 6-31G*) level of theory were carried out to confirm stationary points as minima and to obtain the zero-point energies and the thermal correlation data at 1 atm and 298 K.

Minimal inhibitory concentration (MIC) assay

According to the method described previously [19], MICs was observed in sterilized 96-well polypropylene microtiter plates in a final volume of 200 µl of culture medium. All four of the *S. aureus* strains (5×10^5 CFU/ml) were cultured overnight in 100 µl of broth. Mueller–Hinton (MH) broth, then 100 µl of the culture medium with the test compound (0.12–256 µg/ml in serial twofold dilutions), or with control antibiotics were added into the 96-well plates. After being incubated at 37 °C for 20 h in an incubator, 50 µl of 0.2 % triphenyl tetrazolium chloride (TTC) was added to each well and incubated at 35 °C for 1.5 h. The TTC-based MIC was determined as the lowest concentration that showed no red color change indicating complete growth inhibition. The data were from three repeated experiments.

Bacterial growth inhibition

Bacterial growth inhibition was determined by the time–kill curves according to the published method [20]. In the four *S. aureus* strains culture medium, compound 2 was added to the culture medium to a final concentration of 8, 16, or 32 μg/ml. The bacteria were then cultivated in the automated Bioscreen C system (Lab Systems, Helsinki, Finland) in 300 μl working volume in the wells at 35 °C, which comprised 150 μl MH broth and 150 μl compound 2 solution. The optical density of the bacterial suspensions was measured automatically at 600 nm, which indicates the concentration of bacterial during the 24-h culture period. Statistical data for each experiment were obtained from three independent assays performed in duplicate.

Results

Molecular structure

The crystal structures of compounds 4 and 6 are given in Fig. 2. In the crystal structure of compound 4, a methylene group links two identical 4-hydroxycoumarin moieties and one hydrogen atom is replaced with a 5-bromo-thiophene group. Additionally, a hydroxyl group and a lactone carbonyl group from the two identical 4-hydroxycoumarin molecules, respectively, constitute two classical asymmetrical intramolecular H-bonds, which further stabilized its entire structure [$d(O_2—O_6) = 2.667$ and $d(O_3—O_5) = 2.610$ Å].

In the crystal structure of compound 6, the newly formed pyran ring is essentially planar because the C_3 atom makes a maximum deviation from the C_1-O_1-C_5 plane of 0.7058 Å. The adjacent ketone ring is also essentially planar because the C_7 atom makes a maximum deviation of 0.5621 Å from the C_5-C_4-C_9 plane. The thiophene ring makes a 89.519° angle with the pyran ring plane, and the atoms C_{14} deviate from that plane by 2.6938 Å.

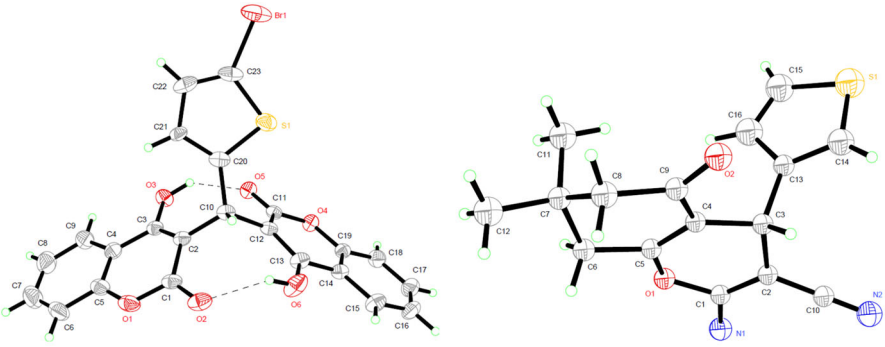

Fig. 2 Crystal structures of compounds 4 and 6

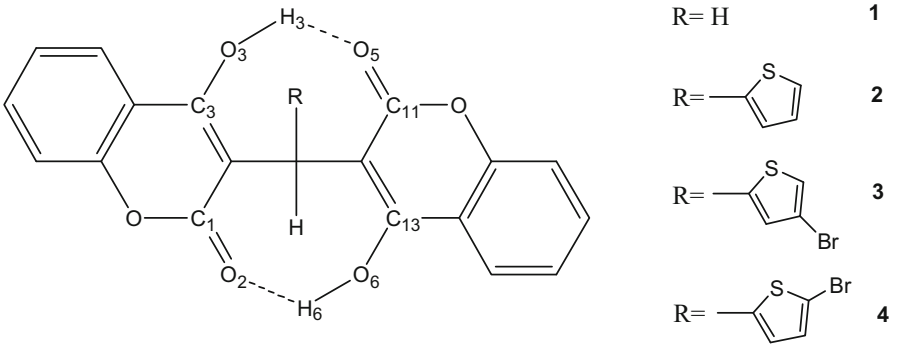

Fig. 3 Schematic presentation of compounds 1–4

Table 2 Experimental and calculated parameters of the selected bond lengths and bond angles of compound 4

Name definition	X-ray	6-31G*	6-31 + G**	6-311G*
C_{11}–O_5	1.215	1.230	1.233	1.222
C_1–O_2	1.215	1.233	1.236	1.226
C_1–O_1	1.351	1.372	1.370	1.371
C_{11}–O_4	1.365	1.375	1.372	1.374
C_2–C_{10}	1.515	1.526	1.526	1.526
C_{12}–C_{10}	1.520	1.527	1.526	1.526
C_{10}–C_{20}	1.519	1.521	1.521	1.520
O_1–C_1–O_2	116.16	115.74	115.94	115.99
O_4–C_{11}–O_5	114.73	115.77	115.93	116.04
C_1–C_2–C_{10}	114.58	114.14	114.10	113.95
C_{11}–C_{12}–C_{10}	118.04	118.88	119.02	118.67
C_2–C_{10}–C_{12}	114.32	113.52	113.71	113.62
C_2–C_{10}–C_{20}	113.06	114.50	114.70	114.64
C_{12}–C_{10}–C_{20}	113.69	113.94	113.89	113.94
C_1–C_2–C_{10}–C_{20}	138.76	134.25	133.62	134.07
C_{11}–C_{12}–C_{10}–C_{20}	51.51	50.07	50.53	50.46
C_1–C_2–C_{10}–C_{12}	89.05	92.54	92.85	92.48
C_{11}–C_{12}–C_{10}–C_2	80.39	83.40	83.38	83.33

Quantum chemical calculations

Geometric parameters of compounds 1–4

The fully optimized molecular structures of compounds 1–4 with atomic numbering calculated at B3LYP level of theory are shown in Fig. 3. For compound 4, selected calculated geometric parameters under three different basis sets and experimental geometric parameters is presented in Table 2.

From Table 2, we can see that the values under three different basis sets are very close, which also agree with the experimental findings. Between theoretical and experimental data, the average discrepancy of the selected bond lengths is $<\pm$ 0.02 Å, and the average discrepancy of the selected bond angles is $<\pm$ 2°. B3LYP/6-31G* showed sufficient agreement with experimental data and lower computational cost, so further theoretical study was performed at this level.

Estimation of the single and total HB energies in compounds 1–4

We take compound 4 for example to estimate single and total HB energies. In compound 4, a global minimum structure is stabilized by two HBs (4ab) and two higher energy structures is stabilized by one HB (4a and 4b), respectively.

The O_6—H_6···O_2 HB energy was calculated to be −52.399729 kJ/mol from the energy difference between 4ab and 4a by the equation $E(O_6—H_6\cdots O_2) = E_{4ab}^{coor} - E_{4a}^{coor}$, in which 4a is a global minimum structure with one HB (O_3—H_3···O_5). Similarly, the O_3—H_3···O_5 HB energy was calculated to be −71.130046 kJ/mol by the equation $E(O_3—H_3\cdots O_5) = E_{4ab}^{coor} - E_{4b}^{coor}$, in which 4b was obtained from the global minimum structure of 4ab, but H_3 was rotated around the C_3—O_3 bond until O_3—H_3···O_5 HB rupture occurred. We can see that O_3—H_3···O_5 HB strength is stronger than that of O_6—H_6···O_2, which is consistent with the fact that the distance of O_3—O_5 (2.610 Å) is shorter than that of O_6—O_2 (2.667 Å). The total HB energy in compound 4 was estimated to be −123.529775 kJ/mol by the equation $2E_{4ab}^{coor} - (E_{4a}^{coor} + E_{4b}^{coor})$. The total HB energy in compounds 1–3 is −119.160943, −125.4805215 and −122.274786 kJ mol^{-1}, respectively (Table 3).

Table 3 Total electronic energies (in hartree) and HB energies (in kJ/mol) of hydrogen bonded conformers of compounds 1–4 calculated at B3LYP/6-31G* level of theory

System	Total electronic energies[a]	E (O_6—H_6···O_2)	E (O_3—H_3···O_5)	E (total HB)
1ab	−1,182.371051			−119.160943
1a	−1,182.348358	−59.5804715		
1b	−1,182.348358		−59.5804715	
2ab	−1,734.116678			−125.4805215
2a	−1,734.096324	−53.439427		
2b	−1,734.089239		−72.0410945	
3ab	−4,305.229694			−122.274786
3a	−4,305.209554	−52.87757		
3b	−4,305.203262		−69.397216	
4ab	−4,305.225972			−123.529775
4a	−4,305.206014	−52.399729		
4b	−4,305.19888		−71.130046	

[a] ZP corrected

Table 4 MIC of compounds 1–6 and antibiotics in Mueller−Hinton broth culture

Drugs	MIC (μg/ml)			
	S. aureas (ATCC 29213)	MRSA (XJ 75302)	Mu50 (ATCC 700699)	LAC (USA 300)
Compound 1	>256	>256	>256	>256
Compound 2	4–8	4–8	8–16	16–32
Compound 3	32–64	32–64	32–64	64–128
Compound 4	32–64	32–64	32–64	64–128
Compound 5	>256	>256	>256	>256
Compound 6	>256	>256	>256	>256
Ceftazidime	8 (S)	>256 (R)	256 (R)	64 (R)
Ceftriaxone	2 (S)	>256 (R)	256 (R)	32 (R)
Gentamicin	0.12 (S)	64 (R)	32 (R)	0.25 (S)
Piperacillin	2 (S)	>128 (R)	>128 (R)	64 (R)

S drug susceptibility, *R* drug resistance

Minimal inhibitory concentration (MIC) assay

One drug-sensitive *S. aureus* (*S. aureus* ATCC 29213) strain and three MRSA strains (MRSA XJ 75302, Mu50, USA 300 LAC) were used in the systematic analysis of the antibacterial activities of compounds 1–6 in vitro, as is shown in Table 4. Compared with dihydropyran derivatives 5 and 6, biscoumarins 1–4 have better bactericidal effects against the four types of *S. aureus* strains, especially for compound 2 with the MIC values of 4–32 μg/ml. Compared with the MIC values of the above compounds, the MIC values of ceftazidime, ceftriaxone, gentamicin, and piperacillin against *S. aureus* (ATCC 29213) strains were lower (<8 μg/ml) but were higher against resistant strains at varying degrees.

Bacterial growth inhibition

Because of the minimum MIC values in compound 2, the growth rate of *S. aureus* in liquid medium containing the different concentrations (8, 16, or 32 μg/ml) were further determined. Compared with compound 2 exhibiting almost completely growth inhibition on these pathogens at 16 or 32 μg/ml, other compounds hardly showed any inhibitory effects at these concentrations (data was not shown), which is consistent with the results of the MIC values. *S. aureus* growth in MH broth without any compounds, which was used as the control sample, did not exhibit any significant growth inhibitory effect. This experiment was repeated three times and the typical result was shown in Fig. 4.

Discussion

Due to the emergence of vancomycin-resistant *S. aureus* and treatment failure of MRSA infections, new antimicrobials need to be developed urgently. In this work,

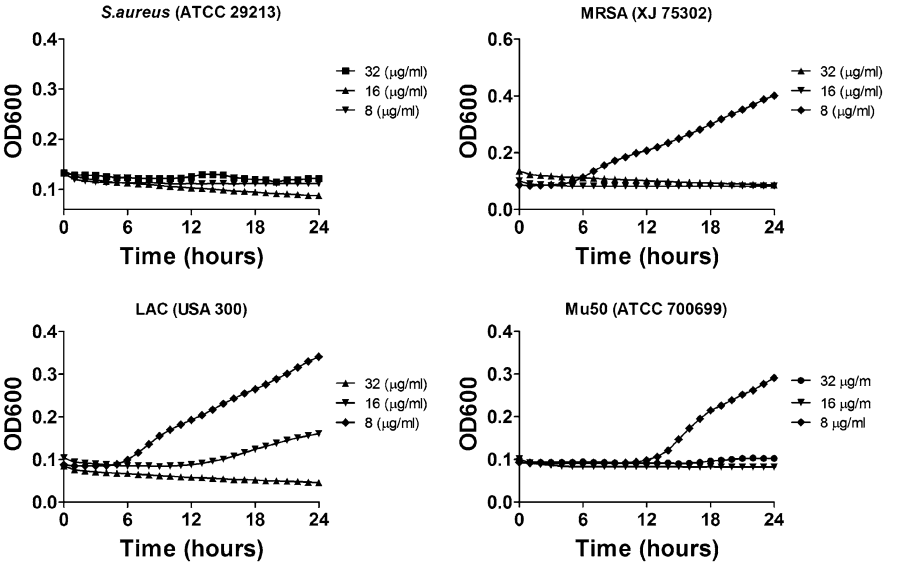

Fig. 4 Concentration-dependent inhibition of compound 2 on the growth of four *S. aureus* strains

we successfully synthesized biscoumarin and dihydropyran derivatives, and then studied their in vitro antibacterial activities.

Both MIC and bacterial growth inhibition results showed that compound 2 exerting potent bactericidal effects against four *S. aureus* strains tested. However, compared with compound 2, other compounds exerted almost no effect on any *S. aureus*.

Two intramolecular O–H···O HBs in the biscoumarins 1–4 were considered as an important factor for biological activity by assisting the molecule to attain the correct configuration. The calculated results are creditable because of the fully optimized molecular structure of compound 2 calculated at B3LYP level of the theory using three different basis sets (6-31G*, 6-31 + G**, and 6-311G*) were in agreement with its available X-ray data.

The total HB stabilization energies in compounds 1–4 were estimated to be −119.160943, −125.4805215, −122.274786, and −123.529775 kJ/mol, respectively. The values in compounds 2–4 are all higher than that of compound 1 because of the effect of thiophene group; the value in compound 2 is higher than those of compounds 3 and 4 because of the effect of bromine atom. These values suggest that the most potent antibacterial activity in compound 2 is consistent with the stronger HB strengths.

Conclusions

With the emergence of methicillin-resistant, vancomycin-intermediate resistant, or multi-drug resistant *S. aureus*, more appropriate antibiotics should be developed.

Our results showed that in the six compounds, compound 2 had the most potent antibacterial efficiency, possibly because 2-thiophene groups on the methylene group further strengthen the HB strengths. To further define the mechanism of antibacterial activity in vivo, additional experiments should be carried out.

Acknowledgments This work was supported by grants from the Industrial Research Project of Science and Technology Department of Shaanxi Province (No. 2013K09-25), National Natural Science Foundation of China (No. 81001460 and No. 81273555) and Innovation Plan of Science and Technology of Shaanxi Province (2014KTCL03-03). The authors thank the High Performance Computing Center of Tianjin University and Prof. Xuehao He for the services provided.

References

1. F. Barbier, A. Andremont, M. Wolff, L. Bouadma, Curr. Opin. Pulm. Med. **19**, 216 (2013)
2. M.W. Climo, D.S. Yokoe, D.K. Warren, T.M. Perl, M. Bolon, L.A. Herwaldt, R.A. Weinstein, K.A. Sepkowitz, J.A. Jernigan, K. Sanogo, E.S. Wong, N. Engl, J. Med. **368**, 533 (2013)
3. P.N. Malani, JAMA **309**, 1408 (2013)
4. V.M. Dukic, D.S. Lauderdale, J. Wilder, R.S. Daum, M.Z. David, PLoS one **8**, e52722 (2013)
5. P.S. Pottinger, Med. Clin. North Am. **97**, 601 (2013)
6. B. Tarai, P. Das, D. Kumar, J. Lab Physicians **5**, 71 (2013)
7. F. Borges, F. Roleira, N. Milhazes, E. Uriarte, L. Santana, Front. Med. Chem. **4**, 23 (2009)
8. Z. Nowakowska, Eur. J. Med. Chem. **42**, 125 (2007)
9. S.K. Ray, S. Rout, V.K. Singh, Org. Biomol. Chem. **11**, 2412 (2013)
10. M.R. Lambu, S. Kumar, S.K. Yousuf, D.K. Sharma, A. Hussain, A. Kumar, F. Malik, D. Mukherjee, J. Med. Chem. **56**, 6122 (2013)
11. N.G. Rokof'eva, N.K. Utkina, E.L. Chaikina, A.E. Makarchenko, Comp. Biochem. Physiol. B Biochem. Mol. Biol. **139**, 167 (2004)
12. C.A. Kontogiorgis, D.J. Hadjipavlou-Litina, J. Med. Chem. **48**, 6400 (2005)
13. H. Eshghi, G.H. Zohuri, R. Sandaroos, S. Damavandi, Heterocycl. Commun. **18**, 67 (2012)
14. G.M. Sheldrick, *SHELXL-97, Program for Solution Crystal Structure and Refinement* (University of Göttingen, Gottingen, 1997)
15. M.J. Frisch, G.W. Trucks, H.B. Schlegel et al., *Gaussian 09, Revision A.02* (Gaussian Inc., Wallingford, 2009)
16. W. Kohn, L.J. Sham, Phys. Rev. **140**, A1133 (1965)
17. A.D. Becke, J. Chem. Phys. **98**, 5648 (1993)
18. C. Lee, W. Yang, R.G. Parr, Phys. Rev. B **37**, 785 (1988)
19. Clinical and Laboratory Standards Institute, *Performance Standards for Antimicrobial Susceptibility Testing: Nineteenth Informational Supplement M100-S19* (Wayne, PA, 2009)
20. M. Motyl, K. Dorso, J. Barrett, Current Protocols in Pharmacology. (Wiley-Liss, New York, 2005) 13A.3.1-22